# Power Loss Calculation Using the Parametric Magneto-Dynamic Model of Soft Magnetic Steel Sheets

Martin Petrun[1], Vojko Podlogar[1], Simon Steentjes[2], Kay Hameyer[2], and Drago Dolinar[1]

[1]Institute of Power Engineering, FERI, University of Maribor, Maribor SI-2000, Slovenia
[2]Institute of Electrical Machines, RWTH Aachen University, Aachen D-52062, Germany

**This paper deals with the fundamental theoretical background of a 1-D parametric magneto-dynamic (PMD) model, which analytically solves the interdependence of the magnetic field and macroscopic eddy currents inside a thin soft magnetic steel sheet (SMSS). Furthermore, the loss calculation using the discussed model is presented, where instantaneous powers due to static hysteresis and induced eddy currents, as well as their power loss distributions across the SMSS thickness are calculated. The calculated results are validated by measurements on a non-oriented SMSS using sinusoidal excitations within wide frequency and magnetic flux density ranges.**

***Index Terms*— Dynamic modeling, eddy currents, loss separation, magnetic hysteresis, power loss, skin effect, soft magnetic materials.**

## I. Introduction

THE widespread usage of non-oriented (NO) soft magnetic steel sheets (SMSSs) in different electromagnetic (EM) devices requires adequate descriptions of EM phenomena inside used SMSSs. Over recent decades, various models have been developed for this purpose, which can predict transient behavior and power losses inside SMSSs. The more established models are based on the numerical solution of the Maxwell diffusion equation, whereas attempts to solve the problem have been done with 1-D [1]–[4], 2-D [5], or even coupled with 3-D [6] approximations. The latter approaches are, however, generally complicated and computationally expensive. Consequently, the main approaches for use in engineering often represent various simplified descriptions for the loss calculation (see [7]) and 1-D problem descriptions. When using the 1-D problem description, some alternative approaches have also been developed, e.g., using magnetic equivalent circuits [8], and most recently, the analytical parametric description of SMSSs [9].

The objective of this paper is twofold. First, to provide a detailed presentation of the fundamental theoretical background, which complements the description of the parametric magneto-dynamic (PMD) model presented in [9]. The detailed presentation for filling the gap in the description of the model is essential for understanding the proposed concepts and is also indispensable for the implementation and further development of the discussed model. Second, to extend the discussed model using the calculations of power losses, as well as power loss distributions inside SMSSs, which are of great importance for enhancing the usability of the discussed model throughout engineering. The calculation of power losses is validated by measurements of a NO SMSS within wide frequency and magnetic flux density ranges.

Manuscript received March 7, 2014; revised April 18, 2014; accepted May 1, 2014. Date of current version November 18, 2014. Corresponding author: M. Petrun (e-mail: martin.petrun@um.si).

Color versions of one or more of the figures in this paper are available online at http://ieeexplore.ieee.org.

Digital Object Identifier 10.1109/TMAG.2014.2323015

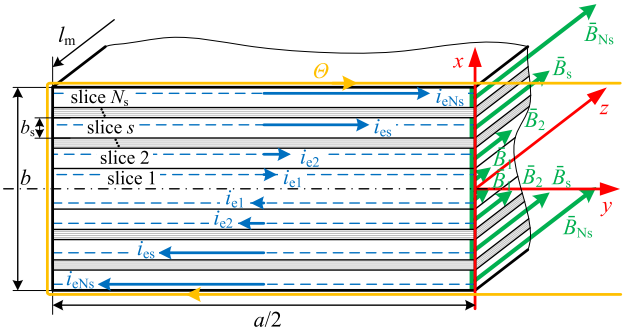


Fig. 1. Left-half side of a thin and long straight SMSS divided into $N_s$ slices.

## II. Parametric Magneto-Dynamic Model

The magnetization dynamics inside a thin and long SMSS is described by the PMD model presented in [9], where the 1-D approximation of the EM phenomena is assumed inside the SMSS.

### A. Theoretical Background of the 1-D Description

A SMSS, which is excited by an external (surface) magnetomotive force (mmf) $\Theta$, e.g., generated by the current $i$ flowing through an excitation winding with $N$ turns ($\Theta = i \cdot N$), is shown in Fig. 1. Although not explicitly indicated, all the used EM variables in this paper represent arbitrary functions of time $t$. For the purpose of the present analysis, a reference coordinate system in the center of the cross section of the SMSS is defined, as shown in Fig. 1. The area of interest for the analysis of the EM field is restricted to the thickness $b$ ($x \in [-b/2,\ b/2]$), width $a$ ($y \in [-a/2,\ a/2]$), and length $l_m$ ($z \in [0,\ l_m]$) of the observed SMSS.

The observed SMSS can be treated as infinitely long, when the length $l_m$ of the SMSS is far greater than its thickness $b$ and width $a (l_m \gg a,\ b)$. In such cases, the magnetic field on the edges has a negligible effect on the magnetic field inside the SMSS. Furthermore, it is assumed that the generated magnetic field inside the SMSS can be represented only

by its component in the direction of the $z$-axis, whereas other components are neglected. Consequently, the EM phenomena inside the SMSS can be considered independent of the $z$ coordinate. The distributions of magnetic field strength $H_z(x, y)$ and magnetic flux density $B_z(x, y)$ across the cross section ($xy$ plane) of the observed SMSS depend, however, on the excitation dynamics and material properties. Such a magnetic field induces, according to Faraday's Law (1), electric field strength $\mathbf{E} = (E_x(x, y),\ E_y(x, y),\ 0)$ in the $xy$ plane. The induced electric field strength is fully described by its components $E_x$ and $E_y$ in the $x$-direction and $y$-direction, respectively,

$$\frac{\partial E_y(x, y)}{\partial x} - \frac{\partial E_x(x, y)}{\partial y} = -\frac{\partial B_z(x, y)}{\partial t}. \tag{1}$$

Due to the induced electric field strength $\mathbf{E}$ and electrically conductive nature of the SMSSs, circular eddy currents $\mathbf{i}_e = (i_{ex}(x, y),\ i_{ey}(x, y),\ 0)$ are generated in the $xy$ plane of the SMSS. The distribution of induced eddy currents depends on the distribution of the varying magnetic field. At the same time, the induced eddy currents influence back the magnetic field. The strong interdependence of the said phenomena can result in non-homogeneously distributed magnetic field and eddy currents inside an SMSS.

Since the thickness $b$ of the SMSS is considerably smaller than its width $a$ ($b \ll a$), the eddy currents $i_{ex}(x, y)$ are considerably smaller than the eddy currents $i_{ey}(x, y)$ and do not substantially influence the magnetic field distribution inside the discussed SMSS. The eddy currents are thus described only by the eddy currents $i_{ey}(x, y)$ directed along the $y$-axis, whereas the $x$-component $i_{ex}(x, y)$ is neglected ($i_{ex}(x, y) = 0$).

Based on aforementioned assumptions, the EM phenomena in the 1-D description are independent of the coordinates $y$ and $z$, and are thus fully represented by magnetic field strength $H = H_z(x)$, magnetic flux density $B = B_z(x)$, and eddy currents $i_e = i_{ey}(x)$. Furthermore, the distribution of the magnetic field and eddy currents along the $x$-axis is symmetric with respect to the $y$-axis (Fig. 1). Due to this symmetry, the diffusion problem can be simplified and solved only for half the thickness of the SMSS [1]–[3].

### *B. Interdependence of Magnetic Field and Eddy Currents*

The main idea of the PMD model proposed in [9] is that the SMSS is divided into several equally thick slices, as shown in Fig. 1. The first slice ($s = 1$) is assumed to be in the center and the last slice ($s = N_s$) close to the surface of the SMSS. The adequate number of slices $N_s$ ($N_s \in \mathbb{N}$) is chosen according to the excitation dynamics in such a way that the otherwise non-uniform distribution of the magnetic field across the SMSS thickness can be described as uniform inside the slices [9]. The magnetic field inside the arbitrary slice $s \in [1,\ N_s]$ is best described by its average values of magnetic field strength $\bar{H}_s$ and magnetic flux density $\bar{B}_s$ (2), where the thickness $b_s$, the lower border coordinate $x_{sl}$, and the upper border coordinate $x_{su}$ of the slice $s$ are defined by

$$\bar{H}_s = \frac{1}{b_s}\int_{x_{sl}}^{x_{su}} H_s(x)\,dx, \quad \bar{B}_s = \frac{1}{b_s}\int_{x_{sl}}^{x_{su}} B_s(x)\,dx \tag{2}$$

$$b_s = \frac{b}{2N_s} \qquad x_{sl} = \frac{(s-1)\,b}{2N_s} \qquad x_{su} = \frac{sb}{2N_s} \tag{3}$$

$$\bar{B}_s = \mu_s(\bar{H}_s)\bar{H}_s. \tag{4}$$

The average magnetic field strength and magnetic flux density (2) in slice $s$ are linked by the constitutive law (4) describing the material properties of the SMSS. The relation between $\bar{H}_s$ and $\bar{B}_s$ is hysteretic and highly non-linear, which can be taken into account using an adequate hysteresis model. For this purpose, various static hysteresis models can be implemented within the discussed model. In this paper, the static hysteresis model proposed in [10] was implemented for several practical reasons [9]. However, for the analysis of complex magnetizations, the use of history-dependent hysteresis models would be more adequate, e.g., the model proposed in [1].

Using an adequate number of slices $N_s$, virtually any arbitrary continuous distribution functions $H(x)$ and $B(x)$ of the magnetic field across the SMSS thickness are adequately approximated with piecewise constant functions $H_{pwc}(x)$ and $B_{pwc}(x)$, which are composed of average values (2) inside individual slices along the $x$-axis. This property of the discussed approximation is essential, as the magnetic field distribution inside the SMSS is changing non-linearly over time, with possible abrupt and significant changes. The eddy current density distribution $j_e(x)$ across the SMSS thickness is calculated by (5) using the piecewise constant approximation $B_{pwc}(x)$ combined with the constitutive Ohm's law and the Faraday's induction law (1)

$$j_e(x) = -\sigma \int_0^x \frac{\partial B_{pwc}(\xi)}{\partial t} d\xi. \tag{5}$$

Using (5) and (2), the eddy current density distribution $j_{es}(x)$ in the arbitrary slice $s$ is calculated by (6). The eddy current density $j_{es}(x)$ at arbitrary position $x$ inside the slice $s$ is generated by the varying magnetic fields within all the embraced inner slices [first term on the right-hand side of (6)] and by that part of the varying magnetic field in slice $s$ that is enclosed inside the observed eddy current density loop at position $x$ (second term on the right-hand side of the following equation):

$$j_{es}(x) = -\sigma b_s \sum_{i=1}^{s-1} \frac{d\bar{B}_i}{dt} - \sigma \frac{d\bar{B}_s}{dt}(x - x_{sl}). \tag{6}$$

In contrast to piecewise constant approximation of the magnetic field distribution $B_{pwc}(x)$, the corresponding approximation of eddy current distribution $j_e(x)$ is according to (6) piecewise linear across the SMSS thickness. By integrating $j_{es}(x)$ (6), the eddy current distribution $i_{es}(x)$ is obtained inside the slice $s$

$$\begin{aligned} i_{es}(x) &= l_m \int_{x_{sl}}^{x} j_{es}(\xi)\,d\xi \\ &= -\sigma l_m \left( b_s \sum_{i=1}^{s-1} \frac{d\bar{B}_i}{dt}(x - x_{sl}) + \frac{1}{2}\frac{d\bar{B}_s}{dt}(x - x_{sl})^2 \right). \end{aligned} \tag{7}$$

The total eddy current $i_{es}$ in the observed slice $s$ is calculated by considering $x = x_{su}$ in (7)

$$i_{es} = -\sigma l_m b_s^2 \left( \sum_{i=1}^{s-1} \frac{d\bar{B}_i}{dt} + \frac{1}{2}\frac{d\bar{B}_s}{dt} \right). \tag{8}$$

Using (7) and considering the total eddy currents in all the inner slices by (8), the average eddy current $\bar{i}_{\mathrm{es}}$ in slice $s$ is expressed as a linear combination of total eddy current $i_{\mathrm{es}}$ in slice $s$ and all total eddy currents in the inner slices by

$$\bar{i}_{\mathrm{es}} = \frac{1}{b_{\mathrm{s}}} \int_{x_{\mathrm{sl}}}^{x_{\mathrm{su}}} i_{\mathrm{es}}(x)\, dx = \frac{1}{3} i_{\mathrm{es}} - \frac{1}{3} \sum_{i=1}^{s-1} (-1)^{s+i}\, i_{\mathrm{e}i}. \quad (9)$$

Up to this point, only the influence of magnetic field distribution on the eddy currents inside the SMSS is analyzed. However, the generated eddy currents create a feedback influence on the magnetic field. This feedback influence is taken into account using Ampere's Law, where the mmf balance within the arbitrary slice $s$ is expressed by (10). The magnetic field at the position $x$ inside the observed slice $s$ is excited by the externally applied mmf $\Theta$, the eddy currents in those slices that enclose slice $s$ [second term on the right-hand side of (10)], and the part of the eddy current in slice $s$ enclosing the observed magnetic field (last two terms on the right-hand side of the following equation):

$$H_{\mathrm{s}}(x)\, l_{\mathrm{m}} = \Theta + \sum_{i=s+1}^{N_{\mathrm{s}}} i_{\mathrm{e}i} + (i_{\mathrm{es}} - i_{\mathrm{es}}(x)). \quad (10)$$

Integrating (10) over the thickness $b_{\mathrm{s}}$ of the observed slice, (10) is expressed in terms of average magnetic field by

$$\frac{1}{b_{\mathrm{s}}} \int_{x_{\mathrm{sl}}}^{x_{\mathrm{su}}} H_{\mathrm{s}}(x)\, l_{\mathrm{m}} dx = \frac{1}{b_{\mathrm{s}}} \int_{x_{\mathrm{sl}}}^{x_{\mathrm{su}}} \left( \Theta + \sum_{i=s+1}^{N_{\mathrm{s}}} i_{\mathrm{e}i} + (i_{\mathrm{es}} - i_{\mathrm{es}}(x)) \right) dx. \quad (11)$$

When analyzing (11), it is easy to identify that the left-hand side of the equation can be replaced by the average magnetic field strength (2) (which is dependent on the average flux density), whereas the right-hand side of (11) can be expressed as the sum of externally applied mmf $\Theta$ and a linear combination of eddy currents within all slices by using (9). The modified formulation of (11) is finally expressed by

$$\bar{H}_{\mathrm{s}}(\bar{B}_{\mathrm{s}}) l_{\mathrm{m}} = \Theta + \sum_{i=s+1}^{N_{\mathrm{s}}} i_{\mathrm{e}i} + \frac{2}{3} i_{\mathrm{es}} + \frac{1}{3} \sum_{i=1}^{s-1} (-1)^{s+i} i_{\mathrm{e}i}. \quad (12)$$

Despite the relatively complicated derivation process, it is interesting that the interdependence of the eddy currents and the magnetic field within the whole SMSS (by considering all the slices) is expressed by a relative simple non-linear differential equation in matrix form (13), as shown in [9]. In (13), $\bar{\mathbf{H}}(\bar{\mathbf{\Phi}})$ represents a vector of the magnetic field strengths as non-linear (hysteretic) functions of the magnetic fluxes inside individual slices, $\mathbf{\Theta}$ is the vector of the mmfs generated by the externally applied current $i$, $\mathbf{N} = N\,[1]_{N_{\mathrm{s}} \times 1}$ is a vector with number of turns $N$ of the excitation winding, and $\mathbf{L}_{\mathrm{m}}$ is the magnetic inductance matrix of the SMSS

$$\mathbf{\Theta} = \mathbf{N} i = \bar{\mathbf{H}}(\bar{\mathbf{\Phi}}) l_{\mathrm{m}} + \mathbf{L}_{\mathrm{m}} \frac{d\bar{\mathbf{\Phi}}}{dt}. \quad (13)$$

The description of the discussed model is completed by the influence of EM phenomena inside the SMSS on the excitation winding. The induced voltage $u_{\mathrm{i}}$ in the excitation winding is generated by time varying magnetic flux densities in all slices and is calculated by

$$u_{\mathrm{i}} = -\mathbf{N}^{\mathrm{T}} \frac{d\bar{\mathbf{\Phi}}}{dt}. \quad (14)$$

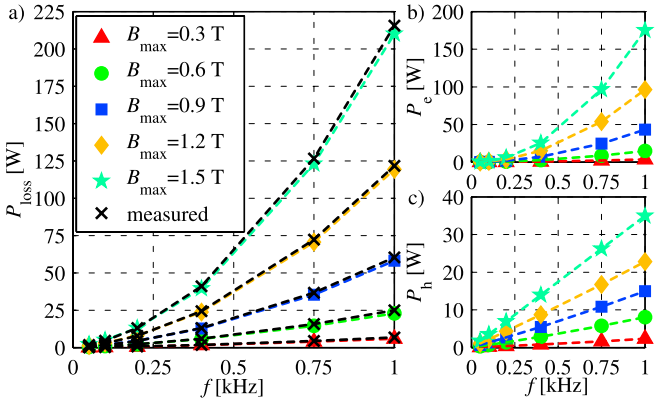


Fig. 2. Power loss inside the M400-50A SMSS. (a) Calculated versus measured total power loss. (b) Calculated eddy current power loss $P_{\mathrm{e}}$. (c) Calculated hysteresis power loss $P_{\mathrm{h}}$.

### C. Power Loss Calculation

Using the discussed model not only the arbitrary transient states (as presented in [9]), but also the power loss distributions inside the SMSSs are calculated, where the time behavior of the powers due to static hysteresis effects and eddy currents are calculated within individual slices of the SMSS.

The total instantaneous conduction power loss $p_{\mathrm{es}}$ due to eddy currents within each slice is calculated by integrating the product of the eddy current density $j_{\mathrm{es}}(x)$ and induced electric field strength $E_{\mathrm{s}}(x)$ over the volume $V_{\mathrm{s}}$ of the slice $s$. Using the constitutive Ohm's law and (7), the total instantaneous conduction power loss $p_{\mathrm{es}}$ is expressed by

$$\begin{aligned} p_{\mathrm{es}} &= \int_{V_{\mathrm{s}}} j_{\mathrm{es}}(x)\, E_{\mathrm{s}}(x)\, dV \\ &= \frac{2 a l_{\mathrm{m}}}{\sigma} \int_{x_{\mathrm{sl}}}^{x_{\mathrm{su}}} j_{\mathrm{es}}^2(x) dx \\ &= 2\sigma a l_{\mathrm{m}} b_{\mathrm{s}}^3 \left[ \left( \sum_{i=1}^{s-1} \frac{d\bar{B}_i}{dt} \right)^2 + \left( \sum_{i=1}^{s-1} \frac{d\bar{B}_i}{dt} \right) \frac{d\bar{B}_{\mathrm{s}}}{dt} \right. \\ &\qquad \left. + \frac{1}{3} \left( \frac{d\bar{B}_{\mathrm{s}}}{dt} \right)^2 \right]. \end{aligned} \quad (15)$$

The total instantaneous power $p_{\mathrm{hs}}$ due to static hysteresis in the individual slice $s$ can be calculated irrespective of the used static hysteresis model with

$$p_{\mathrm{hs}} = a b_{\mathrm{s}} l_{\mathrm{m}} \bar{H}_{\mathrm{s}} \frac{d\bar{B}_{\mathrm{s}}}{dt}. \quad (16)$$

Using (15) and (16), energies $W_{\mathrm{es}}$ and $W_{\mathrm{hs}}$ and average powers $P_{\mathrm{es}}$ and $P_{\mathrm{hs}}$ within the time period $\Delta t = (t_2 - t_1)$

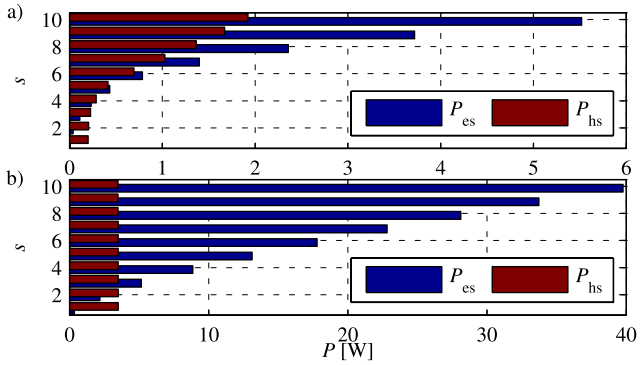


Fig. 3. Power loss distribution inside individual slices $s$ due to eddy currents $P_{\mathrm{es}}$ and static hysteresis $P_{\mathrm{hs}}$ at $f = 1000$ Hz. (a) $B_{\max} = 0.6$ T. (b) $B_{\max} = 1.5$ T.

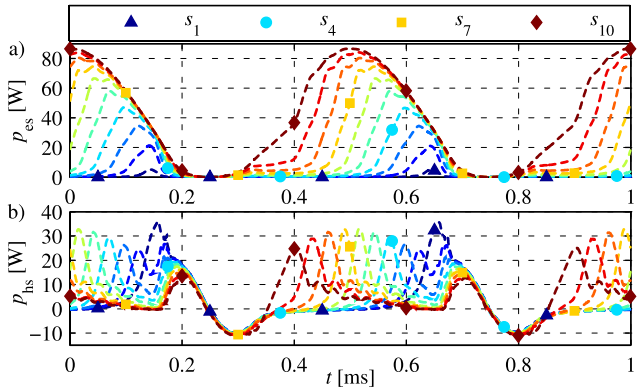


Fig. 4. Calculated instantaneous powers in different slices $s$ for $B_{\max} = 1.5$ T and $f = 1000$ Hz. (a) $p_{\mathrm{es}}$ due to eddy currents. (b) $p_{\mathrm{hs}}$ due to hysteresis.

inside individual slice $s$ can be calculated by

$$P_{\mathrm{es}} = \frac{W_{\mathrm{es}}}{\Delta t} = \frac{1}{\Delta t}\int_{t_1}^{t_2} p_{\mathrm{es}}(t)\,dt \qquad P_{\mathrm{hs}} = \frac{W_{\mathrm{hs}}}{\Delta t} = \frac{1}{\Delta t}\int_{t_1}^{t_2} p_{\mathrm{hs}}(t)\,dt. \tag{17}$$

The total instantaneous powers $p_{\mathrm{e}}$ and $p_{\mathrm{h}}$, energies $W_{\mathrm{e}}$ and $W_{\mathrm{h}}$, and average powers $P_{\mathrm{e}}$ and $P_{\mathrm{h}}$ for the entire SMSS are obtained by summing the components of the individual slices.

## III. Results

In order to overcome the spatial limitation of this paper and provide a comparable, coherent, and complete analysis of the presented PMD model, the loss calculation is validated and presented for the same sample of a M400-50A NO steel and under equal conditions as used in [9].

The presented results are calculated using the same static hysteresis description, $N_{\mathrm{s}} = 10$ slices and a specific electrical conductivity of $\sigma = 2.16 \cdot 10^6$ S/m [9]. The calculated total power losses $P_{\mathrm{loss}}$ show a good agreement with the measurements within the frequency range up to $f = 1000$ Hz by considering the maximum average magnetic flux densities up to $B_{\max} = 1.5$ T [Fig. 2(a)]. The corresponding calculated power losses due to eddy currents and static hysteresis are shown in Fig. 2(b) and (c), respectively. The power loss distribution inside individual slices is shown in Fig. 3, where it is apparent that at lower maximum magnetic flux densities the hysteresis losses are bigger in the outer slices of the SMSS due to the skin effect [Fig. 3(a)]. However, when the SMSS is saturated the hysteresis losses are almost independent of the SMSS depth [Fig. 3(b)]. The dynamics of the calculated instantaneous powers $p_{\mathrm{es}}$ and $p_{\mathrm{hs}}$ in different slices $s$ inside the observed SMSS corresponding to Fig. 3(b) are shown in Fig. 4.

## IV. Conclusion

This paper provides detailed insight into the fundamental theoretical background of the PMD model presented in [9] and expands the discussed model with power loss calculation. The presented analysis complements the analysis presented in [9] and leaves the discussed model open for modifying or including possible additional concepts to account for different phenomena. Besides, the relative simplicity, good computational performance and other advantages [9], with the discussed model the dynamics of power loss components inside the SMSS, as well as power loss distribution across the SMSS thickness can also be calculated. The latter could be used in an advanced model, i.e., using a coupled thermal model of the SMSS, which would influence back the material properties of the SMSS. Future work will focus on implementation and analysis of various static hysteresis models for accurate modeling under arbitrary excitation conditions of the SMSSs.

## Acknowledgment

This work was supported by ARRS under Project P2-0115, Project L2-5489 and Project L2-4114.

## References

[1] S. E. Zirka, Y. I. Moroz, P. Marketos, and A. J. Moses, "Viscosity-based magnetodynamic model of soft magnetic materials," *IEEE Trans. Magn.*, vol. 42, no. 9, pp. 2121–2132, Sep. 2006.

[2] S. E. Zirka, Y. I. Moroz, P. Marketos, and A. J. Moses, "Loss separation in nonoriented electrical steels," *IEEE Trans. Magn.*, vol. 46, no. 2, pp. 286–289, Feb. 2010.

[3] S. Steentjes, F. Henrotte, C. Geuzaine, and K. Hameyer, "A dynamical energy-based hysteresis model for iron loss calculation in laminated cores," *Int. J. Numer. Model., Electron. Netw., Devices Fields*, vol. 27, no. 3, pp. 433–443, 2014.

[4] A. T. Raminosoa, C. Chillet, M. Fassenet, J. Yonnet, and J. Voyant, "An analytical approach of magnetic diffusion in a plate under time-varying flux excitation," *IEEE Trans. Magn.*, vol. 50, no. 4, pp. 1–4, Apr. 2014.

[5] E. Dlala, A. Belahcen, J. Pippuri, and A. Arkkio, "Interdependence of hysteresis and eddy-current losses in laminated magnetic cores of electrical machines," *IEEE Trans. Magn.*, vol. 46, no. 2, pp. 306–309, Feb. 2010.

[6] H. D. Gersem, S. Vanaverbeke, and G. Samaey, "Three-dimensional-two-dimensional coupled model for eddy currents in laminated iron cores," *IEEE Trans. Magn.*, vol. 48, no. 2, pp. 815–818, Feb. 2012.

[7] D. Eggers, S. Steentjes, and K. Hameyer, "Advanced iron-loss estimation for nonlinear material behavior," *IEEE Trans. Magn.*, vol. 48, no. 11, pp. 3021–3024, Nov. 2012.

[8] A. Davoudi, P. L. Chapman, J. Jatskevich, and H. Behjati, "Reduced-order dynamic modeling of multiple-winding power electronic magnetic components," *IEEE Trans. Power Electron.*, vol. 27, no. 5, pp. 2220–2226, May 2012.

[9] M. Petrun, V. Podlogar, S. Steentjes, K. Hameyer, and D. Dolinar, "A parametric magneto-dynamic model of soft magnetic steel sheets," *IEEE Trans. Magn.*, vol. 50, no. 4, pp. 1–4, Apr. 2014.

[10] J. Tellinen, "A simple scalar model for magnetic hysteresis," *IEEE Trans. Magn.*, vol. 34, no. 4, pp. 2200–2206, Jul. 1998.